Boundary Influences on the 7 July 2008 Tornado Event

CHAUNCY J. SCHULTZ
National Weather Service, North Platte, Nebraska

(Manuscript received 18 July 2009; in final form 10 November 2009)

ABSTRACT

A long-track EF3 tornado did significant damage to the north-central North Dakota town of Rolla on 7 July 2008. The parent supercell of this tornado occurred in close proximity to an outflow boundary. Another supercell that interacted with this same boundary later in the afternoon only produced a brief, weak tornado, despite strong low-level gate-to-gate shear and a distinct hook echo. Subtle, but important, temporal and spatial differences in the low-level thermodynamic and kinematic setting may have influenced tornado probability along the boundary. These differences will be investigated and discussed. Finally, a high-resolution, convection-resolving simulation of the Advanced Research core of the Weather Research and Forecasting (WRF-ARW) model will be used to determine whether its output would have helped forecasters anticipate this event.

1. Introduction

Boundaries have been associated with many tornado cases, as noted by Thompson et al. (2008), which found that storm-boundary interactions occurred in 44% of the significant tornado cases they analyzed. Markowski et al. (1998b) suggested that storm-relative helicity (SRH), which has been highly correlated with significant tornadoes (Davies-Jones 1993), may be greatly enhanced in the vicinity of boundaries, "which may supply additional buoyancy-generated streamwise vorticity in environments where only marginal values of SRH for severe storms are indicated." However, Davies-Jones (1993) and Markowski et al. (1998a) have both shown SRH to vary dramatically both spatially and temporally, and have stated that this variability may in part explain why some storms are tornadic and others are not.

Thompson et al. (2008) found that many of the boundary-interaction cases in their study involved only a single significant tornado in a given convective outbreak, rather than multiple

Corresponding author address: Chauncy J. Schultz, National Weather Service, 5250 East Lee Bird Drive, North Platte, NE 69101-2473
E-mail: Chauncy.Schultz@noaa.gov

events. An isolated significant tornado occurred near a boundary in north-central North Dakota on 7 July 2008, when a supercell produced a long-track tornado that caused EF3 damage to the community of Rolla. The supercell originated in southwestern Manitoba around 1900 UTC, and produced two EF0 tornadoes (at 1923 and 1945 UTC) before the Rolla tornado formed around 1950 UTC. The Rolla tornado had a path length of 33.8 km (21 miles) and a maximum width of 0.23 km (250 yards; Fig. 1). The tornado struck the north side of Rolla, North Dakota, at 2030 UTC (Fig. 2). Twelve homes were destroyed and eighteen were damaged in Rolla. Total damage from the 7 July 2008 tornadoes was over 1.5 million dollars (NOAA *Storm Data*).

The primary objective of this paper is to quantify the environment that produced a strong tornado near Rolla, and to use a high-resolution numerical model simulation to determine if its output could have aided in anticipating this mesoscale event. The paper also seeks to investigate why a second supercell that interacted with the same outflow boundary as the Rolla storm failed to produce anything more than a brief, weak tornado.

2. Data collection and methodology

The event is studied using surface, upper-air, and satellite imagery from the National Climatic Data Center (NCDC). The surface observations are supplemented with data from the North Dakota Agricultural Weather Network (NDAWN). Archived radar data from the (WSR-88D) radars in Mayville (KMVX) and Minot (KMBX), North Dakota were also obtained from NCDC. The environment is also analyzed using Rapid Update Cycle (RUC) data at 20-km horizontal resolution, as described by Benjamin et al. (2002). The data are analyzed in the framework of the Storm Prediction Center (SPC) analysis scheme (Bothwell et al. 2002). RUC model soundings are also used, which Edwards and Thompson (2000) have shown to be useful in the evaluation of supercell environments when the RUC is adequately modeling the mesoscale environment. All thermodynamic variables are analyzed using the virtual temperature correction described by Doswell and Rasmussen (1994). Finally, a 4-km horizontal grid spacing (HGS) simulation of the Advanced Research core of the Weather Research and Forecasting model (WRF-ARW; Skamarock and Klemp 2008) will be utilized to determine whether or not this output would have helped forecasters anticipate the tornado.

3. Event Analysis and Discussion

a. Synoptic setting and evolution

Nearly zonal mid- and upper-level flow was present across the continental United States at 1200 UTC 7 July 2008, though a moderate and amplifying short-wave trough was observed across the northern Plains (Fig. 3). The trough continued its eastward propagation and deepening during the next 12-hour period, at which time the left exit region of a 35-40 m s^{-1} 250-hPa jet streak was present over central North Dakota (Figs. 4 and 5).

The approach of the short-wave trough, nocturnal increase in the low-level jet to 10-15 m s^{-1} atop a weak low-level warm front, and resultant warm air advection led to the formation of an MCS over central and eastern North Dakota by 1200 UTC 7 July 2008 (Fig. 6). This MCS exited the state by 1800 UTC. However, an outflow boundary formed in its wake in the vicinity of the weak warm front (Fig. 7). The 1800 UTC surface station plot in Fig. 7 revealed 16-18° C (61-64° F) temperatures on the cool side of the boundary, some 5-8°F cooler than in the warm sector. Positive surface moisture advection was ongoing during the day with dewpoints ranging from 17-20°C (62-68°F) on both sides of the boundary during the afternoon.

The 700-hPa trough line passed through central North Dakota during the midday hours of 7 July 2008 (Figs. 8 and 9). This caused 700-hPa winds to veer with time, while surface winds remained easterly due to cyclonic flow across the outflow boundary. Wind strength also increased aloft and contributed to 30-40 kts of 0–6-km bulk vertical wind shear across central and eastern North Dakota, sufficient for the organization of rotating updrafts, as discussed by Bunkers et al. (2006; Fig. 10). The RUC analysis indicates that a second mid-level short-wave trough (e.g., 700-500 hPa) approached the region after 1800 UTC (not shown), which may have aided convective initiation across central North Dakota and southwest Manitoba.

Visible satellite imagery showed clearing progressing eastward across central North Dakota between 1500 and 1800 UTC (Fig. 11). Strong diabatic heating ensued in the wake of the clearing line; however, the effects of the shallow cool outflow were still notable from north-central through east-central parts of the state. That is, a distinct temperature gradient around 6°C (10°F) remained across the boundary through the afternoon, even though diabatic heating did occur on the cool side of the boundary as clouds from the MCS moved eastward. As a result, the effective outflow boundary began to retreat north-northeastward at a speed near 25 kts between 1800 and 2100 UTC (Fig. 12). The air mass near the boundary heated for several hours before convection regenerated, which may have been key to the formation of intense surface-based updrafts.

Moisture convergence was focused in the vicinity of the outflow boundary near Rolla. Data from the NDAWN station located 3.22 km (2 miles) south of Rolla showed an increase in surface dewpoint from 13.9°C (57°F) at 1600 UTC to 19.4°C (67°F) at 2000 UTC, when the tornadic supercell was approaching the area (Fig. 13). All of this allowed SBCAPE to increase substantially in a relatively narrow corridor east of a surface dryline, and along, south, and west of the outflow boundary. Especially notable was the degree of low-level SBCAPE present near the intersection of the two boundaries, where a favorable juxtaposition of strong diabatic heating, rich low-level moisture, and steep lapse rates existed.

a. The Rolla tornadic supercell environment

The Rolla supercell initiated shortly after 1830 UTC near the “triple point” where the outflow boundary and surface dryline intersected in southwestern Manitoba (Fig. 7). The “triple point” has been associated with many tornado events, such as that described in Weiss and Bluestein (2002). Between 1912 and 1923 UTC, an appendage became evident along the reflectivity gradient on the southern flank of the supercell, when an EF0 tornado occurred near Lake Metigoshe in southwestern Manitoba (not shown). By 2007 UTC, two separate areas experienced rapid increases in gate-to-gate (GTG) shear. One was near the southwestern edge of the deep reflectivity core of the storm, and had a magnitude of 60 kts. However, it is the area that originated within the flanking line, initially displaced from the hook echo that persisted. By 2020 UTC, this feature had maximum GTG shear signature of 80-90 kts at 4400 feet AGL 6.44 km (4 miles) northwest of Rolla. When the rotation passed over Rolla at 2029 UTC, it was maximized in the hook echo of the storm with a magnitude of at least 100 kts (Fig. 14).

A distinct overlap of 0–3-km lapse rates in excess of 7°C km^{-1} and 0-3 km mixed layer CAPE (MLCAPE) over 100 J kg^{-1} was located in north-central North Dakota (Fig. 15). RUC soundings at Rolla show the rapid thermodynamic changes that occurred from 1800 through 2000 UTC (Figs. 16 and 17). The 2000 UTC sounding yielded ~2800 J kg^{-1} of SBCAPE. Impressively, over 300 J kg^{-1} of 0-3-km SBCAPE was present. This large value of low-level SBCAPE suggests enhanced updraft acceleration and stretching in the low levels (Davies 2002).

The small temperature and dewpoint spreads that existed along and east of the outflow boundary also contributed to low LCLs. The RUC analysis data suggest that LCL heights dropped from over 1500 m AGL along the dryline to less than 800 m AGL east of the outflow boundary. In fact, the LCL was 300 m or less in the vicinity of the Rolla supercell when assessed from RUC point soundings. This is below the 25th percentile of the tornadic soundings studied by Rasmussen and Blanchard (1998).

The low-level wind shear was substantial along and east of the outflow boundary. RUC analyses valid from 1800 through 2200 UTC showed around 25 kts of 0–1-km bulk wind shear in that area (Fig. 18), which was similar to the values observed by the KMVX Velocity Azimuth Display (VAD) wind profile (not shown). This is at and above the mean value of 0–1-km bulk wind shear found by Thompson et al. (2002) to be associated with significant tornadoes. The 0–1-km SRH near Rolla was near 150 $m^2\ s^{-2}$. In contrast, the 0-1-km SRH was 50 $m^2\ s^{-2}$ or less on the warm side of the outflow boundary, which is below the 10th percentile of both strong and weak tornado events in the Thompson et al. (2002) study. The lack of strong low-level shear in the warm sector led to a reduced concern for tornadoes early in this event.

The Rolla supercell, with its propagational speed (~30 kts) slightly greater than that of the outflow boundary (~25 kts), likely remained within a similar environment to that noted in the 2000 UTC Rolla sounding (Fig. 17) for a significant amount of time. The storm moved nearly parallel to the isotherms in the vicinity of the boundary, which is one characteristic it has in common to other long-track tornadoes associated with thermal boundaries (Maddox et al. 1980).

b. Interaction of another supercell with the outflow boundary

A particularly interesting event in this case occurred across east-central North Dakota near 2200 UTC. At that time, a supercell crossed the retreating outflow boundary in Steele

County. Shortly after 2200 UTC, the cell developed a distinct weak echo region on its forward flank and a notable hook echo. The 0.5° SRM imagery from KMVX indicated a rapid increase in GTG shear, which was maximized near 100 kts at 500 m (1500 feet) AGL at 2231 UTC (Fig. 19). A brief EF0 tornado was observed in Steele County with this storm at 2230 UTC (NOAA *Storm Data*). The strong GTG shear was not as temporally significant as with the Rolla supercell (Fig. 20). However, its interaction with the same outflow boundary as the Rolla storm, and at least briefly significant radar signatures, beg the question, "*What was different about this environment than that observed near Rolla?*"

RUC analyses from 2100 through 2300 UTC suggest 0–1-km bulk shear remained in excess of 20 kts along and east of the outflow boundary. SRH also remained relatively high near the Steele County storm (~125 $m^2 s^{-2}$), and not that dissimilar from Rolla. However, the *gradient* in 0-1 km SRH shown across the retreating outflow boundary (as suggested by RUC output) was weaker than at the time of the Rolla event (Fig. 21). It is not clear what the difference in SRH gradient may physically mean to a supercell. However, given the strong spatial and temporal variability in SRH noted by Davies-Jones (1993) and Markowski et al. (1998a), it is possible that the stronger gradient seen in 20-km resolution RUC data at the time of the Rolla tornado was merely implying larger values of SRH existed than shown. That is, the RUC data may not capture the SRH maxima, but a stronger gradient may imply that the magnitude of maximum SRH is larger at one time than another. This hypothesis requires much in the way of additional research.

The orientation of the storm motion vector relative to the boundary may have also played an important role in the longevity of its tornado threat, as the Steele County storm continued to move deeper into the cool air and at least slightly less SBCAPE (after crossing the boundary at a nearly normal angle), while in the case of the Rolla storm, the boundary was propagating at a comparable speed to the storm. This likely maintained the same general environment in the vicinity of the Rolla storm for a much longer time, even if the storm was some distance away from the surface boundary. In addition, although total SBCAPE was similar near both supercells, the 0-3 km SBCAPE in Steele County (~180 J kg^{-1}) was 44% less than at Rolla (~320 J kg^{-1}).

c. Potential gravity wave influence on mesoscyclone strength

The animation in Fig. 14 shows a detached and pre-existing area of reflectivity that moved northeast near the inflow region of the Rolla supercell, at a speed slightly faster than the storm. This feature could be a gravity wave. Based on the results of Coleman and Knupp (2008), if this is a gravity wave, it could be responsible for the significant increase in rotation of the Rolla supercell (and thus could be a reason the storm produced a much more intense tornado than the Steele County supercell). Fig. 11 also shows a narrow zone of “billow clouds” (closely and regularly spaced wave-like clouds) east of the outflow boundary before convective initiation. This is indicative of a shallow, stable boundary layer, and given the strong low-level shear, this situation was favorable for gravity wave production and maintenance (Holton 1992). Interestingly, the animation in Fig. 19 shows a reflectivity feature ahead of the Steele County storm, as well, which also moved northeast faster than the supercell. However, this feature emanated from another storm not discussed herein, and while its interaction with the Steele County storm may have impacted its tornado potential, it likely does not reflect the presence of a gravity wave.

4. High-Resolution Mesoscale Modeling

A high-resolution WRF-ARW simulation was conducted for the case using the numerical model construction utilized at the National Weather Service (NWS) in Marquette, Michigan (Hulquist et al. 2007). The simulation utilized two-way nesting with 12-km HGS in the outer nest and 4-km HGS in the inner nest. Model simulation parameters are summarized in Table 1. The WRF-ARW incorrectly lifted a warm front into southern Manitoba after 1200 UTC, since it did not develop the MCS in its simulation until several hours after its actual occurrence (Fig. 22). Although the position of the modeled warm front is incorrect due to the mistiming of the MCS, it is near the front that forecast SBCAPE is highest (1000-1500 J kg^{-1}) and forecast 0–1-km bulk wind shear is in excess of 20 kts (over at least portions of the frontal segment; not shown).

The 4-km HGS WRF-ARW reflectivity forecast very accurately depicted the development of thunderstorms both along the surface dryline and warm front. The convection that developed on the dryline struggled to survive more than 2-3 hours as it moved into the forecasted low-CAPE environment to its east (not shown). However, the cell forecasted to develop on the warm front does quite the opposite; between 1900 and 2100 UTC the reflectivity forecast suggested a supercell-like structure to this particular cell (Fig. 23). The lifetime of simulated and observed cells was relatively similar, although in reality the dryline-based storms lasted longer than three hours. Impressively, the forecast supercell occurred within one hour and approximately 97 km (60 miles) of the Rolla event. The modeled 0-1-km bulk wind shear also increased to over 30 kts in the area near the modeled supercell (Figs. 23c and 23d). This output could have aided forecasters in anticipating supercell potential in the wake of the morning MCS, although it is not clear if it was the background environment or the simulated supercell that contributed to the strong shear, since both developed nearly simultaneously in the model.

5. Concluding Comments

This event reiterates that not all outflow boundaries (or even different segments of the same outflow boundary) possess the same potential to aid the production of tornadoes. When assessing boundary-related tornado potential, forecasters need to be particularly aware of differences in propagation motion of storms with respect to boundaries. Subtle environmental differences such as the degree of low-level CAPE may also influence tornado probability in these cases. One final interesting aspect of the supercell comparison in this case not explicitly discussed thus far is that the storm that actually *crossed* the boundary was the one that failed to produce a strong tornado. This could imply that it is environmental differences, and not necessarily boundary-induced vorticity itself, that are most important in determining the potential for a stronger or longer-lived boundary-related tornado event. However, it must be noted that in this case the time evolution of the boundary, and variability in its structure at any given time, are not well known.

This event makes a case for being aware of both SRH gradients and potential gravity waves when assessing tornado potential on the mesoscale, all other variables being equal. Neither is necessarily often-considered in real time, but both appeared to at least potentially influence the tornado threat with the Rolla supercell.

Acknowledgements. The author thanks Dr. Mark Askelson, University of North Dakota, Jeff Manion, NWS Central Region Headquarters, Dr. Timothy Coleman and Dr. Kevin Knupp, University of Alabama-Huntsville, and Jeffrey Medlin, NWS Mobile, AL, for their thorough reviews of this paper. The author would also like to thank Mike Dutter, NWS Marquette, MI, for performing the WRF run, as well as Bradley Bramer, NWS Grand Forks, ND, and David Derung, Nathan Heinert, and Joshua Scheck, NWS Bismarck, ND, for collecting data, preparing images, and insightful discussions.

REFERENCES

Benjamin, S. G., and Coauthors, 2002: RUC20-The 20-km version of the Rapid Update Cycle. NOAA Tech. Memo. OAR FSL twenty eight. Forecast Systems Laboratory, Boulder, CO, 9 pp.

Bothwell, P. D., J. A. Hart, and R. L. Thompson, 2002: An integrated three-dimensional objective analysis scheme in use at the Storm Prediction Center. Preprints, *21st Conf. Severe Local Storms*, San Antonio, TX, Amer. Meteor. Soc., 117–120.

Bunkers, M. J., J. S. Johnson, L. J. Czepyha, J. M. Grzywacz, B. A. Klimowski, and M. R. Hjelmfelt, 2006: An observational examination of long-lived supercells. Part II: Environmental conditions and forecasting. *Wea. Forecasting*, **21**, 689–714.

Coleman, T.A., and K.R. Knupp, 2008: The Interactions of Gravity Waves with Mesocyclones: Preliminary Observations and Theory. *Mon. Wea. Rev.*, **136**, 4206–4219.

Davies, J. M., 2002: On low-level thermodynamic parameters associated with tornadic and non-tornadic supercells. Preprints, *21st Conf. Severe Local Storms*, San Antonio, TX, Amer. Meteor. Soc., 603-606.

Davies-Jones, R. P., 1993: Helicity trends in tornado outbreaks. Preprints, *17th Conf. Severe Local Storms*, St. Louis, MO, Amer. Meteor. Soc., 56–60.

Doswell, C.A. III, and E.N. Rasmussen, 1994: The effect of neglecting the virtual temperature correction on CAPE calculations. *Wea. Forecasting*, **9**, 625-629.

Edwards, R., and R.L. Thompson, 2000: RUC-2 Supercell Proximity Soundings, Part II: An Independent Assessment of Supercell Forecast Parameters. Preprints, *20th Conf. Severe Local Storms*, Orlando FL, Amer. Meteor. Soc., 435-438.

Holton, J., 1992: *Dynamic Meteorology*. 3rd Ed. Academic Press, 511 pp..

Hulquist, T. R., J. L. Lee, and M. Zika, 2007: Use of High Resolution WRF-ARW Output at a National Weather Service Forecast Office: The 21 July 2002 and 9 August 2005 Upper Michigan Bow Echo Events. Preprints, *8th WRF Users' Workshop*, Boulder, CO, National Center for Atmospheric Research, online.

Maddox, R., L.R. Hoxit, and C.F. Chappell, 1980: A Study of Tornadic Thunderstorm Interactions with Thermal Boundaries. *Mon. Wea. Rev.*, **108**, 322–336.

Markowski, P. M., J. M. Straka, E. N. Rasmussen, and D. O. Blanchard, 1998a: Variability of storm-relative helicity during VORTEX. *Mon. Wea. Rev.*, **126**, 2959-2971.

--, E. N. Rasmussen, and J. M. Straka, 1998b: The occurrence of tornadoes in supercells interacting with boundaries during VORTEX-95. *Wea. Forecasting*, **13**, 852–859.

NOAA *Storm Data*, 2008: Available from National Climatic Data Center, Asheville, NC 28801.

Rasmussen, E. N., and D. O. Blanchard, 1998: A baseline climatology of sounding-derived supercell and tornado forecast parameters. *Wea.Forecasting*, **13**, 1148-1164.

Skamarock, W.C., and J.B. Klemp, 2008: A time-split non-hydrostatic atmospheric model, *Journal of Computational Physics*, **227**, 3465–3485

Thompson, R.L., R. Edwards, and J.A. Hart, 2002: An Assessment of Supercell and Tornado Forecast Parameters with RUC-2 Model Close Proximity Soundings. Preprints, *21st Conf. Severe Local Storms*, San Antonio, TX, Amer. Meteor. Soc, 595-598.

--, J.S. Grams and J.A. Prentice, 2008: Synoptic Environments and Convective Modes Associated with Significant Tornadoes in the Contiguous United States. Preprints, *24th Conf. Severe Local Storms*, Savannah, GA, Amer. Meteor. Soc, paper 16A.3.

Weiss, C.C., and H.B. Bluestein, 2002: Airborne Pseudo–Dual Doppler Analysis of a Dryline–Outflow Boundary Intersection. *Mon. Wea. Rev.*, **130**, 1207–1226.

TABLES AND FIGURES

Table 1. WRF-ARW version 2.1.2 characteristics.

	12-km HGS outer nest	**4-km HGS inner nest**
Initial/Boundary Conditions	NARR (32 km HGS)	Two-way nesting with 12-km HGS outer grid
Convective Parameterization	Kain-Fritsch	None
Vertical Levels and Model Top	31; 100-hPa	31; 100-hPa
Radiation Scheme (Short/Long Wave)	Dudhia/RRTM	Dudhia/RRTM
Microphysics	Lin et al. (1983)	Lin et al.
Planetary Boundary Layer Scheme	YSU	YSU
Land Surface Model	Noah	Noah

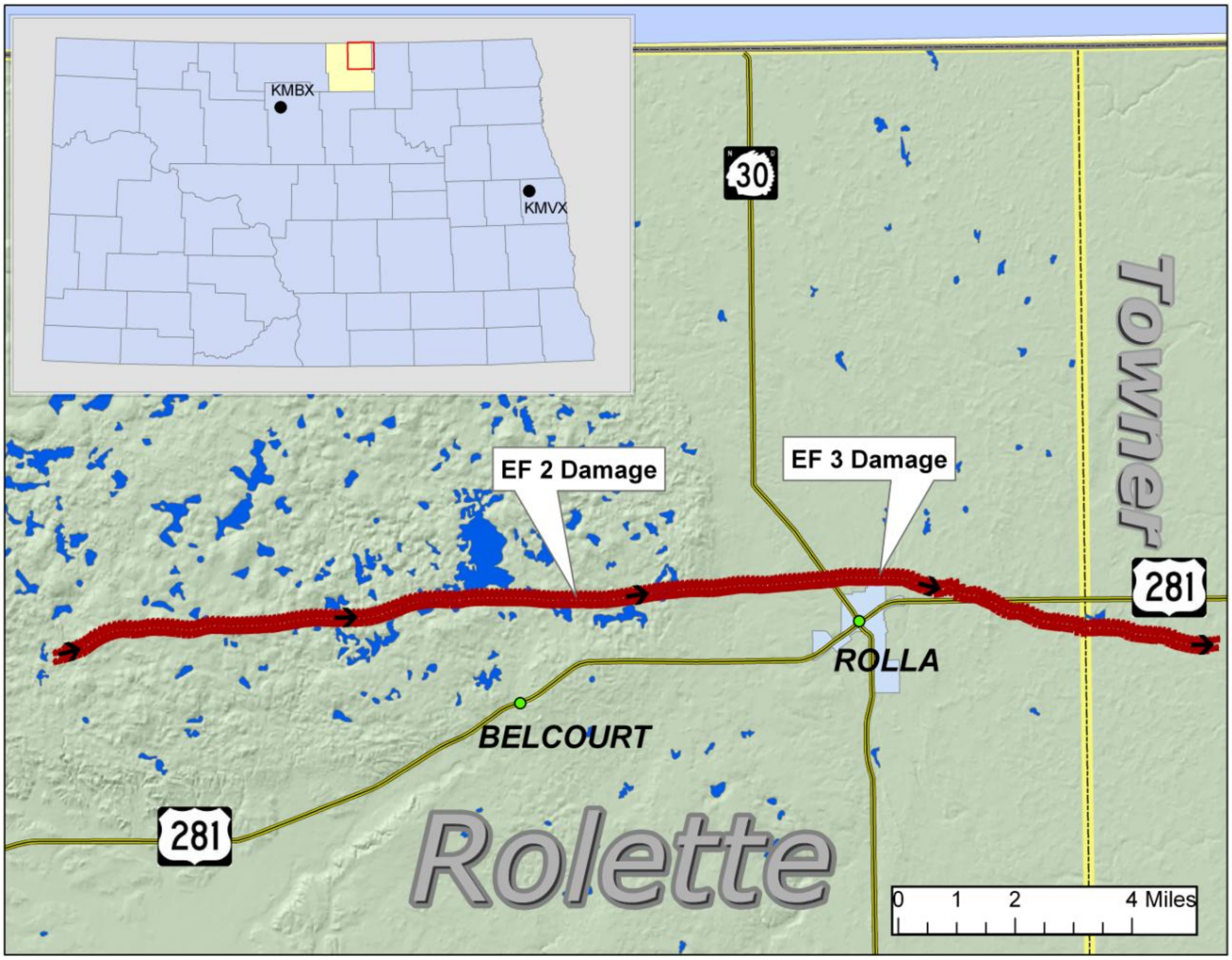

Figure 1. Path of the EF3 tornado in Rolette and Towner Counties, North Dakota (credit: Nathan Heinert).

Figure 2. Photograph of the EF3 tornado in Rolla, North Dakota, near 2030 UTC 7 July 2008 (credit: KXMB Television, Bismarck, North Dakota).

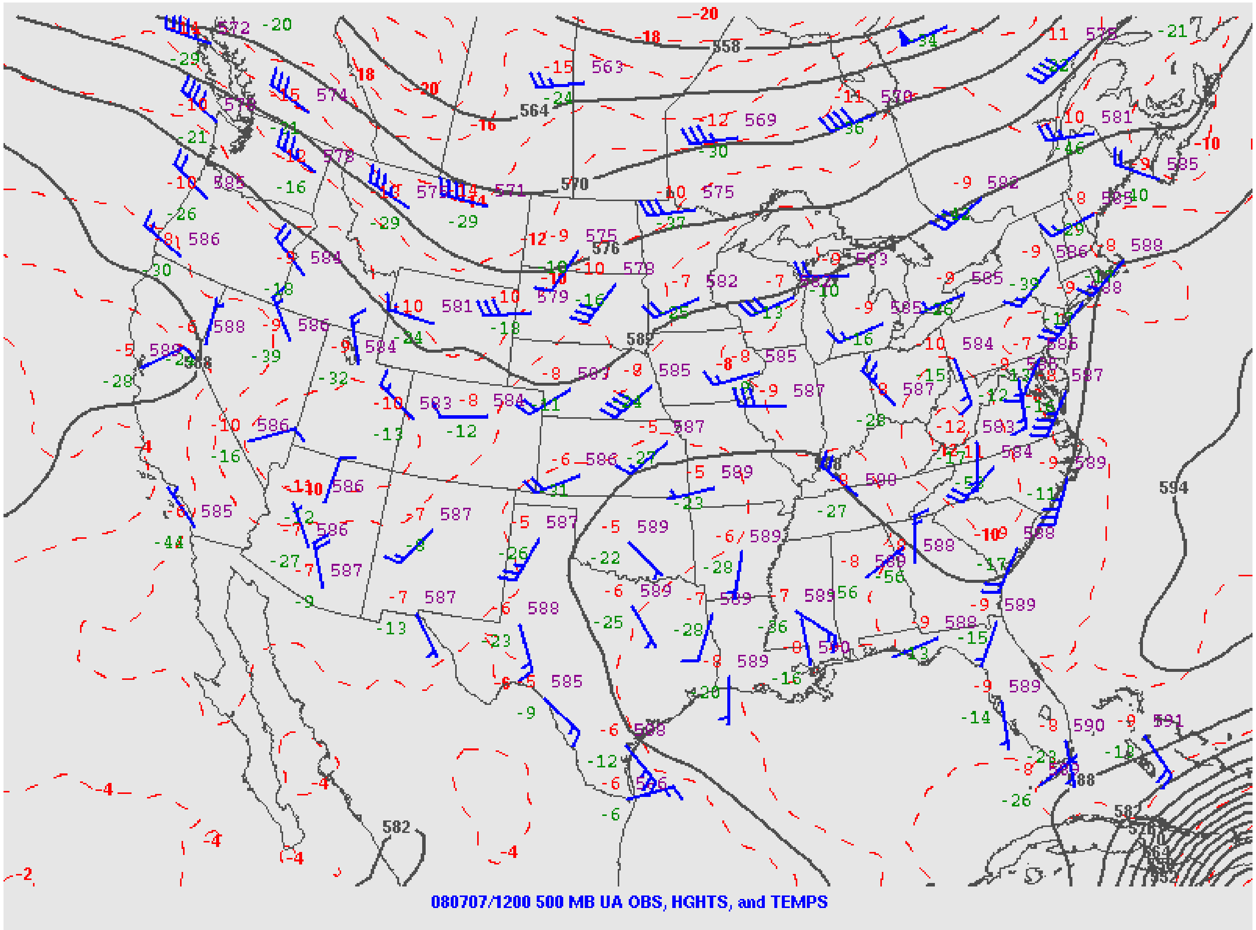

Figure 3. 500-hPa observations (conventional form) at 1200 UTC 7 July 2008 with isotherms [dashed red contours, contour interval (CI) = 2° C] and height contours (solid grey contours, CI = 60 m).

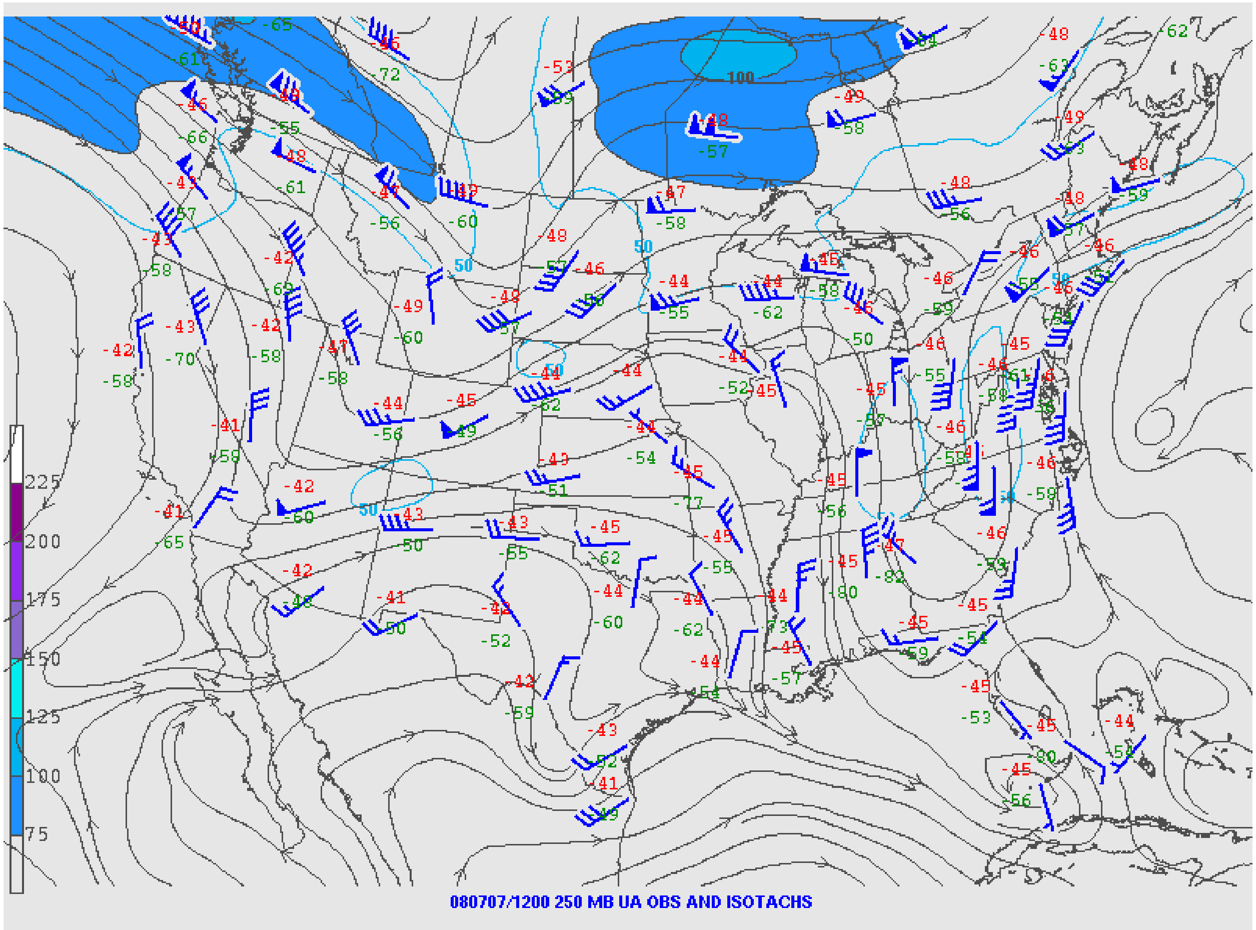

Figure 4. 250-hPa observations in conventional form at 1200 UTC 7 July 2008 with streamlines and isotachs (colored, CI = 25 kts).

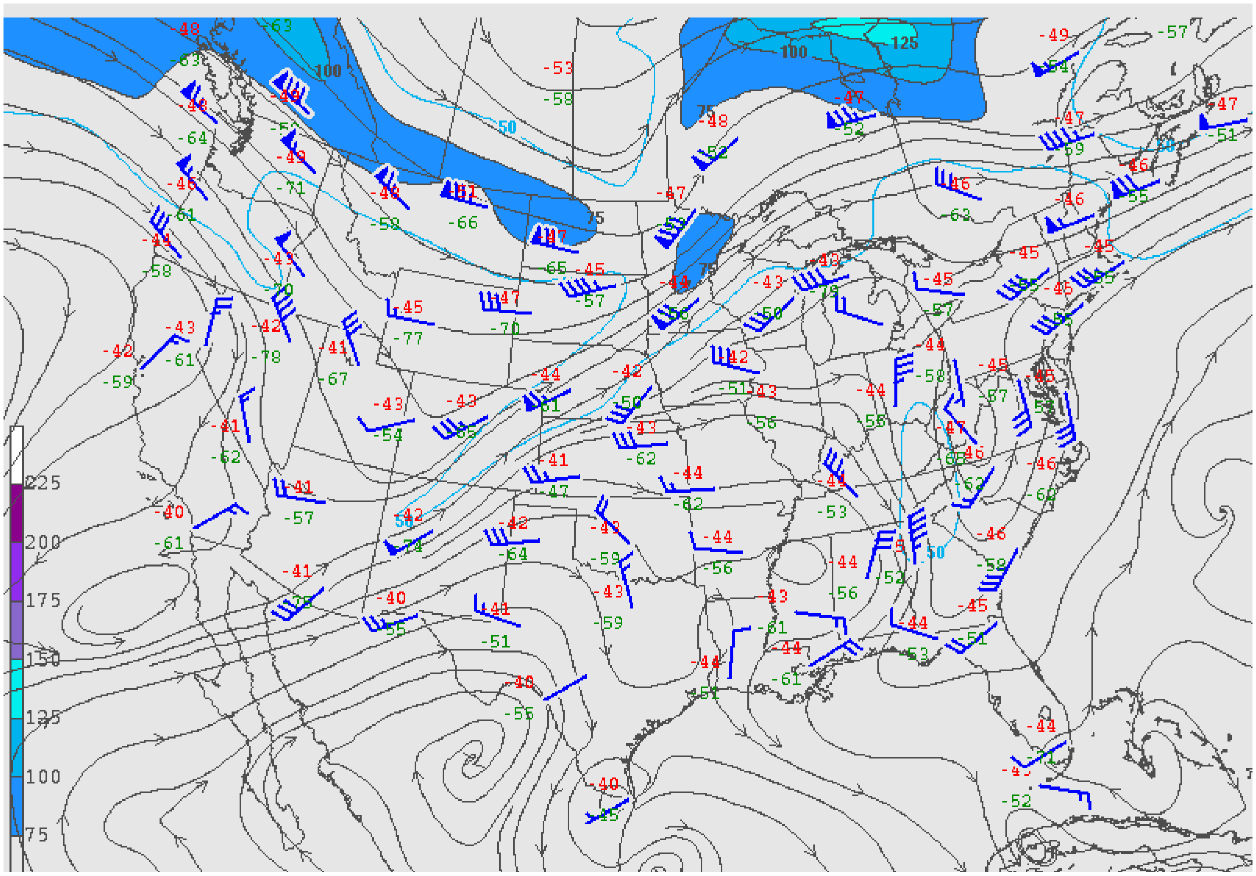

Figure 5. As in Fig. 4 except for 0000 UTC 8 July 2008.

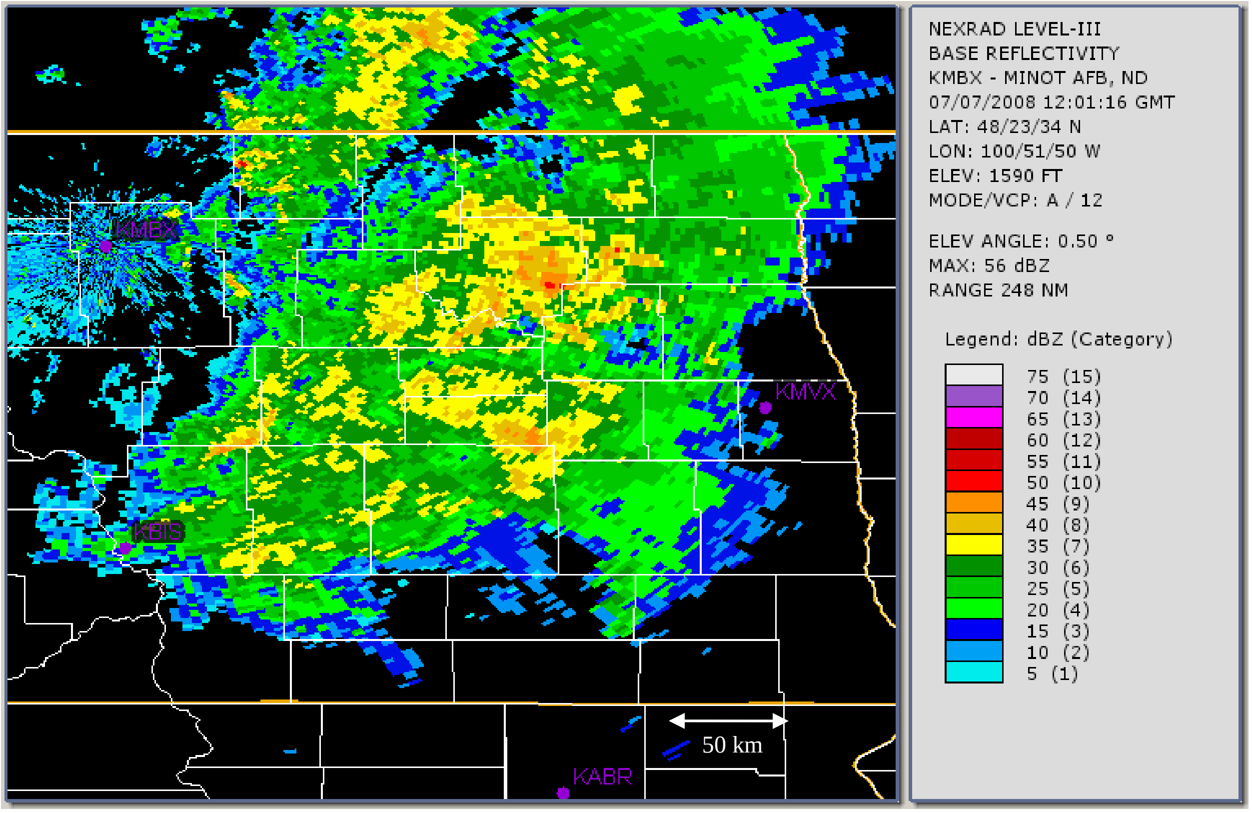

Figure 6. Minot, North Dakota (KMBX) WSR-88D long range 0.5° radar reflectivity imagery at 1201 UTC 7 July 2008. Click here for an animation from 1200 to 1930 UTC 7 July 2008.

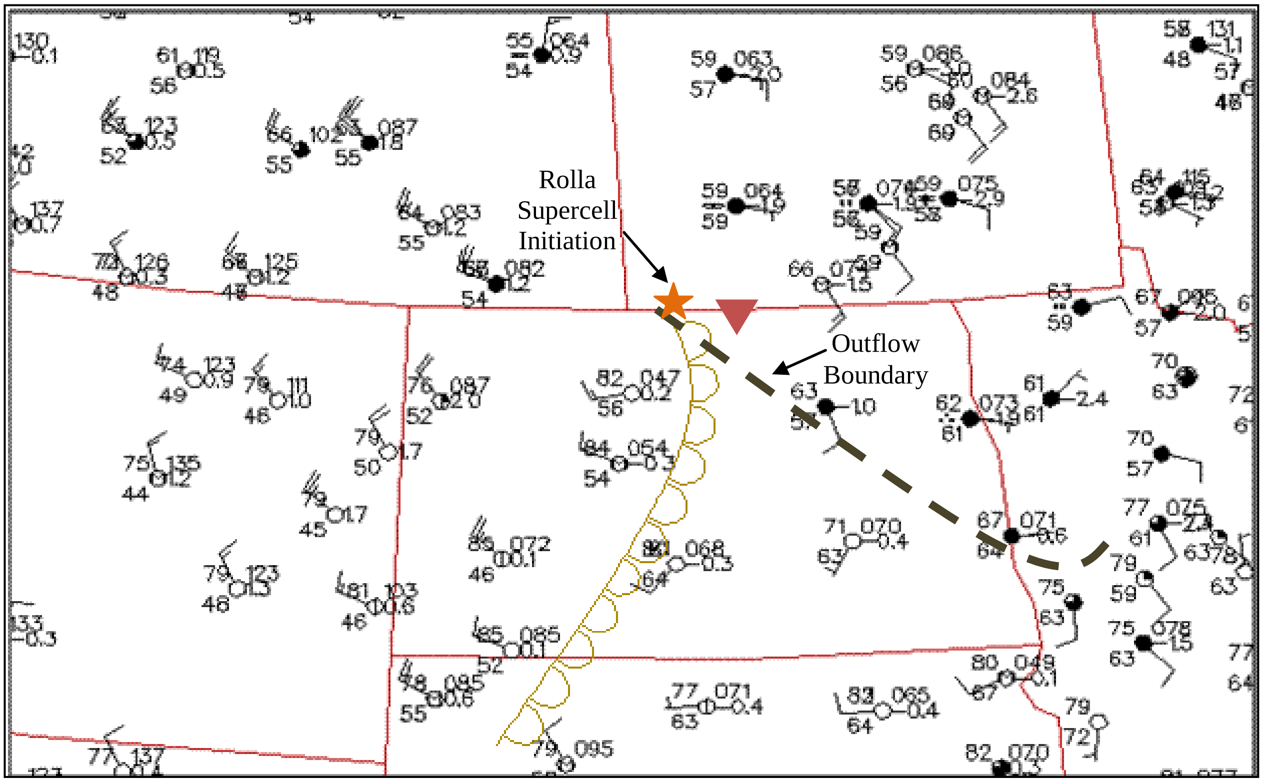

Figure 7. Surface map at 1800 UTC 7 July 2008 with conventional surface observations. Inverted red triangle highlights the location of the Rolla, North Dakota EF3 tornado at 2030 UTC. Dashed purple line represents approximate outflow boundary position. Solid brown represents approximate surface dryline position. Orange star notes initiation point of Rolla supercell around 1830 UTC.

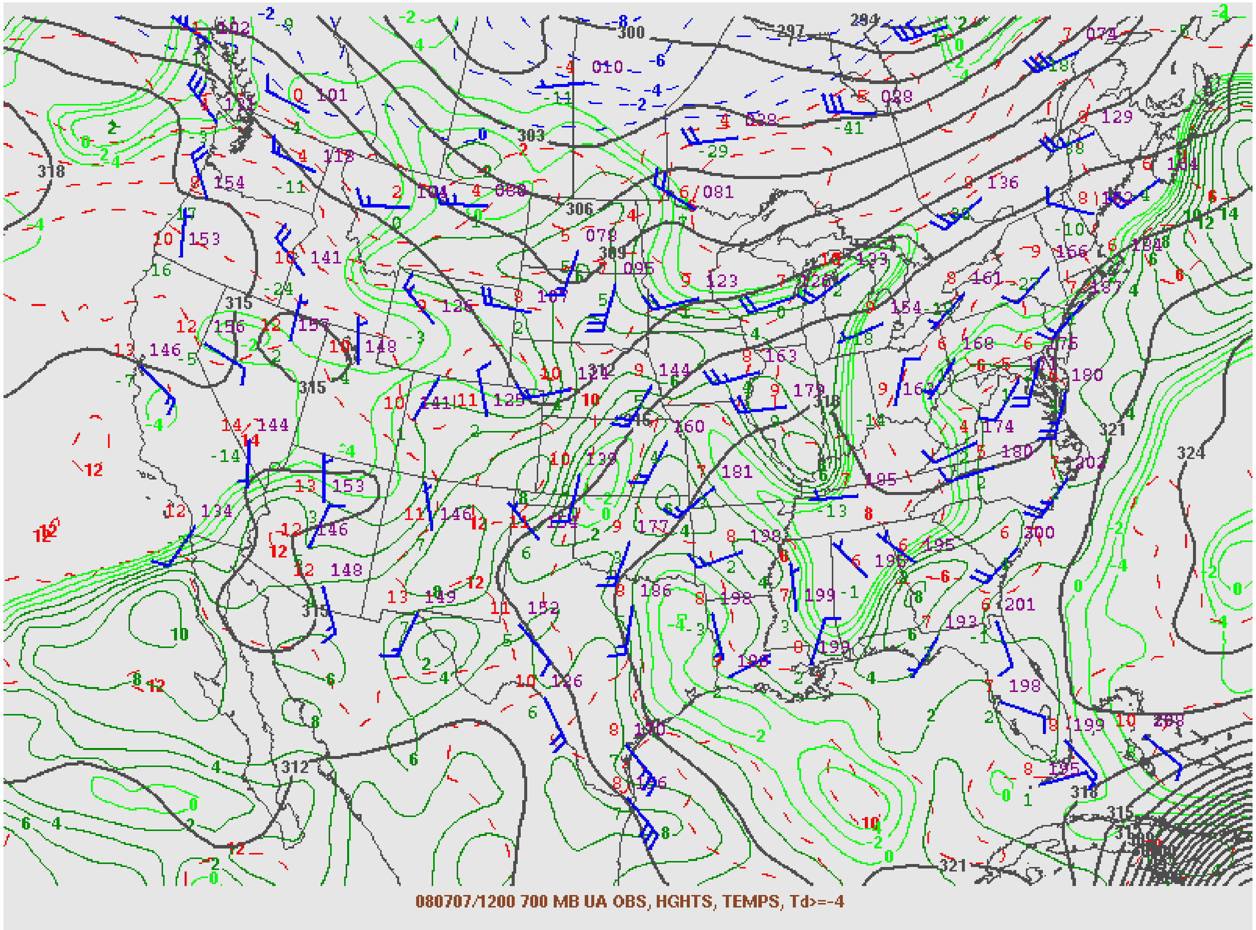

Figure 8. 700-hPa observations in conventional form at 1200 UTC 7 July 2008 with isotherms (dashed red contours, CI = 2° C), isodrosotherms (solid green contours, CI = 2° C), and heights (solid grey contours, CI = 30 m).

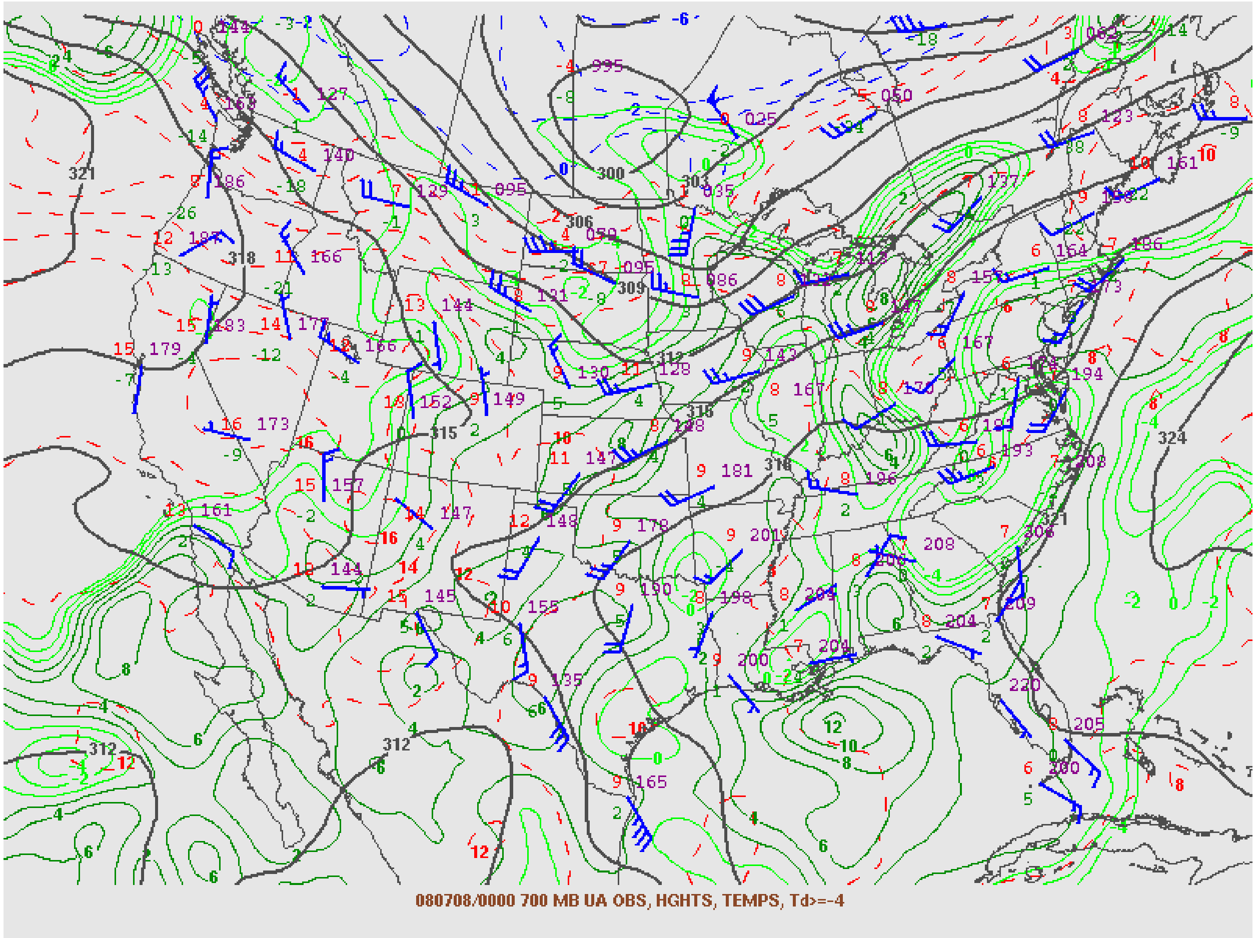

Figure 9. As in Fig. 8 but for 0000 UTC 8 July 2008.

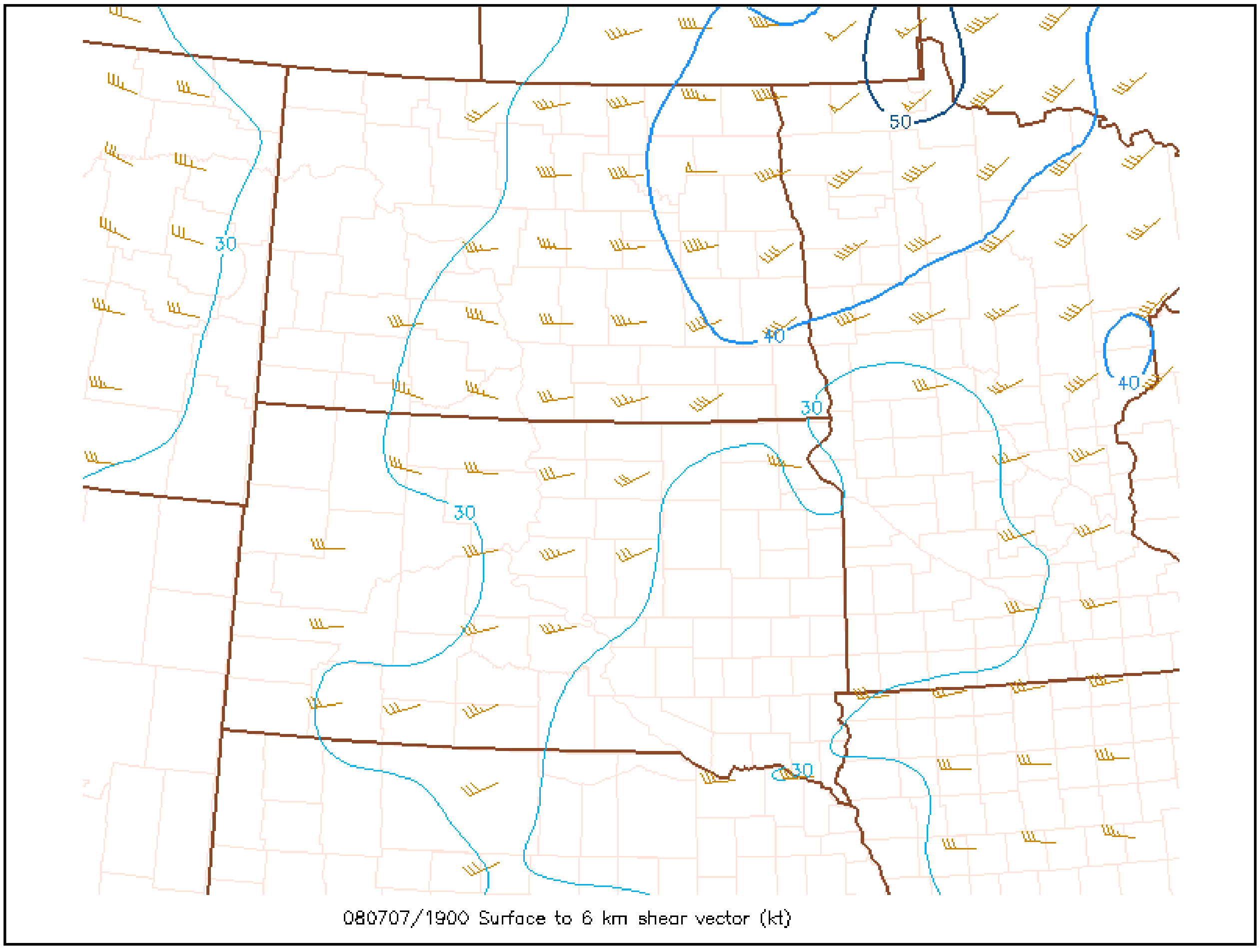

Figure 10. RUC 00-hour analysis of 0–6-km bulk wind shear vectors and magnitude (solid blue contours, CI = 10 kt beginning at 30 kt) at 1800 UTC 7 July 2008.

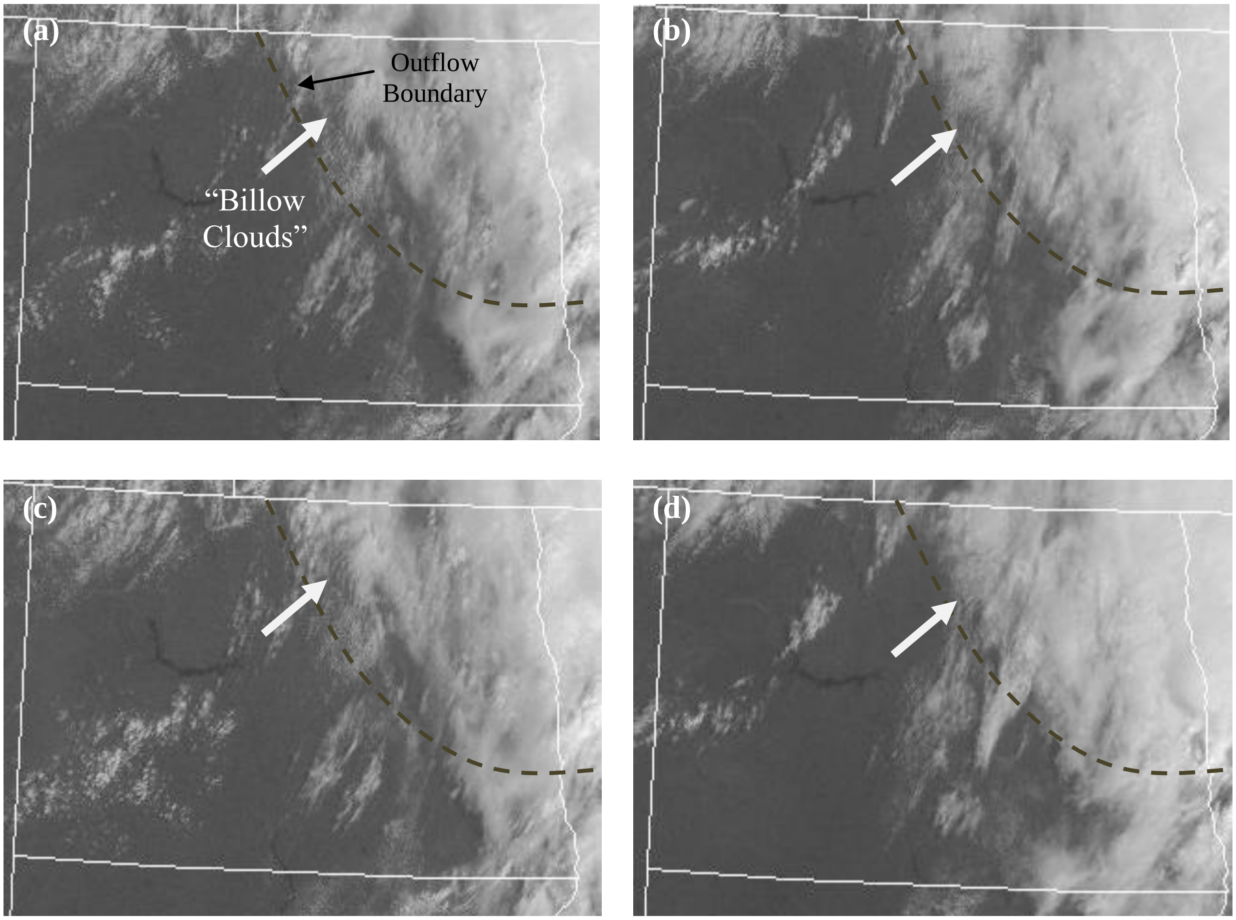

Figure 11. Geostationary Operational Environmental Satellite-12 (GOES-12) visible satellite imagery series on 7 July 2008 at a) 1645 UTC b) 1715 UTC c) 1745 UTC and d) 1800 UTC. White arrows point to billow cloud formations. Brown dashed line marks approximate outflow boundary position.

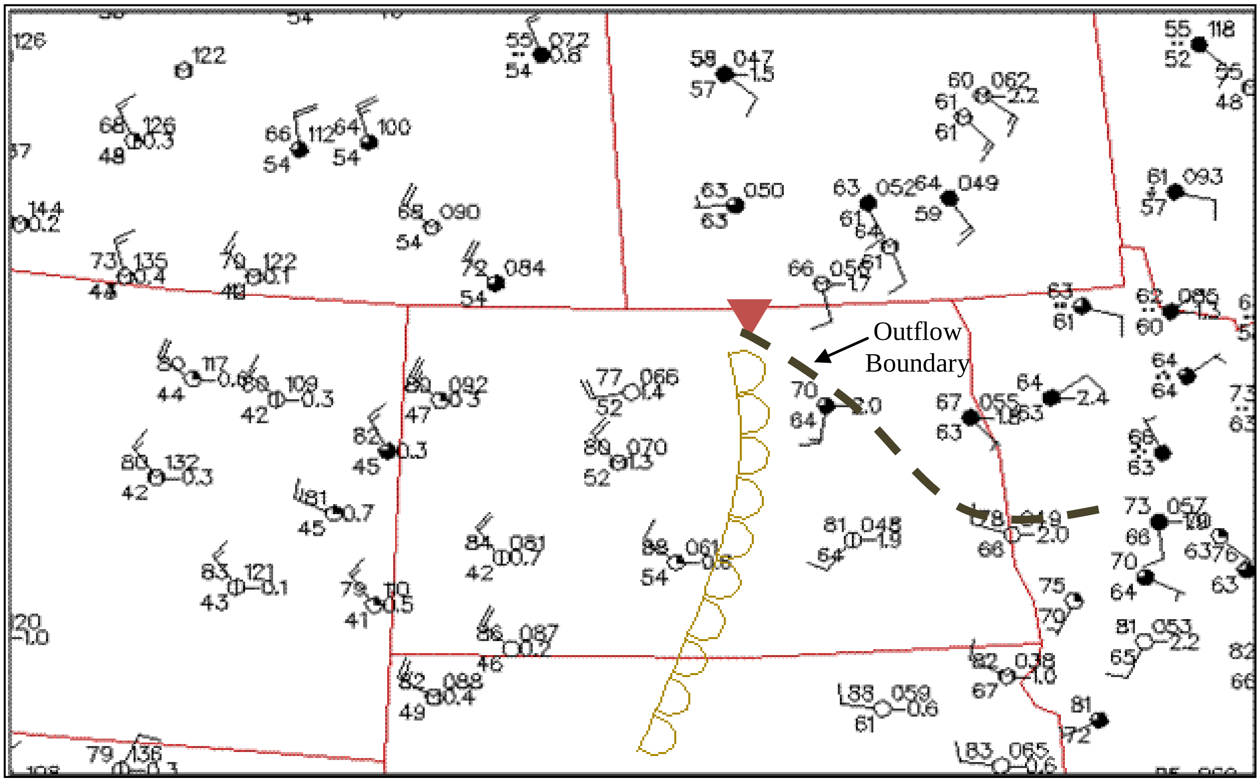

Figure 12. As in Fig. 7 but for 2100 UTC 7 July 2008. Inverted red triangle highlights the location of the Rolla, North Dakota EF3 tornado at 2030 UTC.

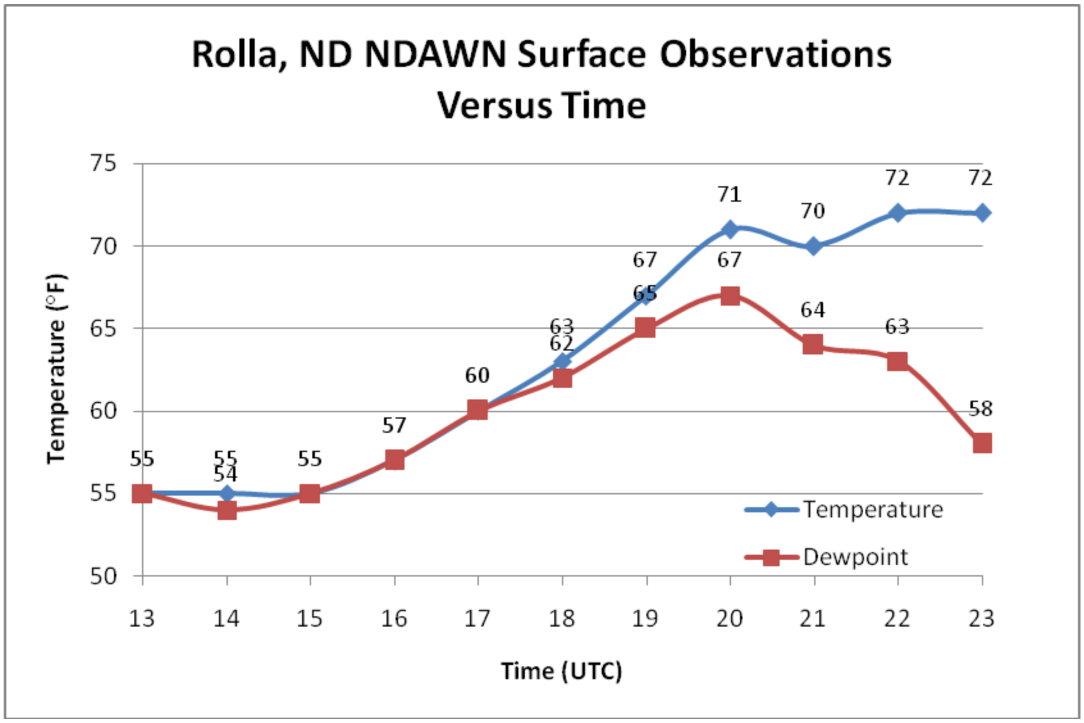

Figure 13. Time series of surface temperature (blue solid line) and dewpoint (red solid line) in °F from 1300 to 2300 UTC 7 July 2008 taken at the Rolla, ND NDAWN station.

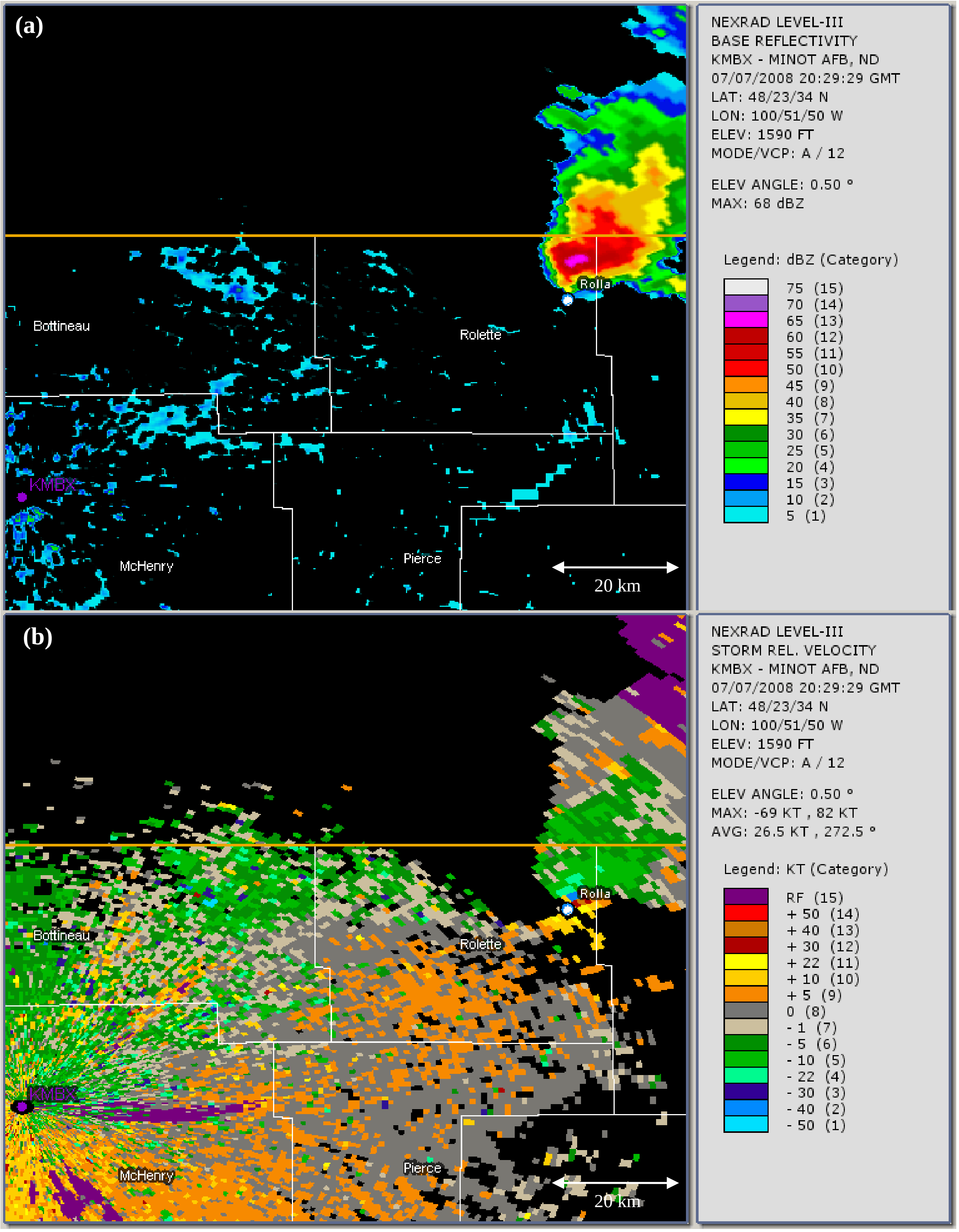

Figure 14. KMBX WSR-88D imagery at 2029 UTC 7 July 2008 for a) 0.5° radar reflectivity and b) 0.5° storm-relative velocity. Click here for an animation of “a” and here for an animation of “b”.

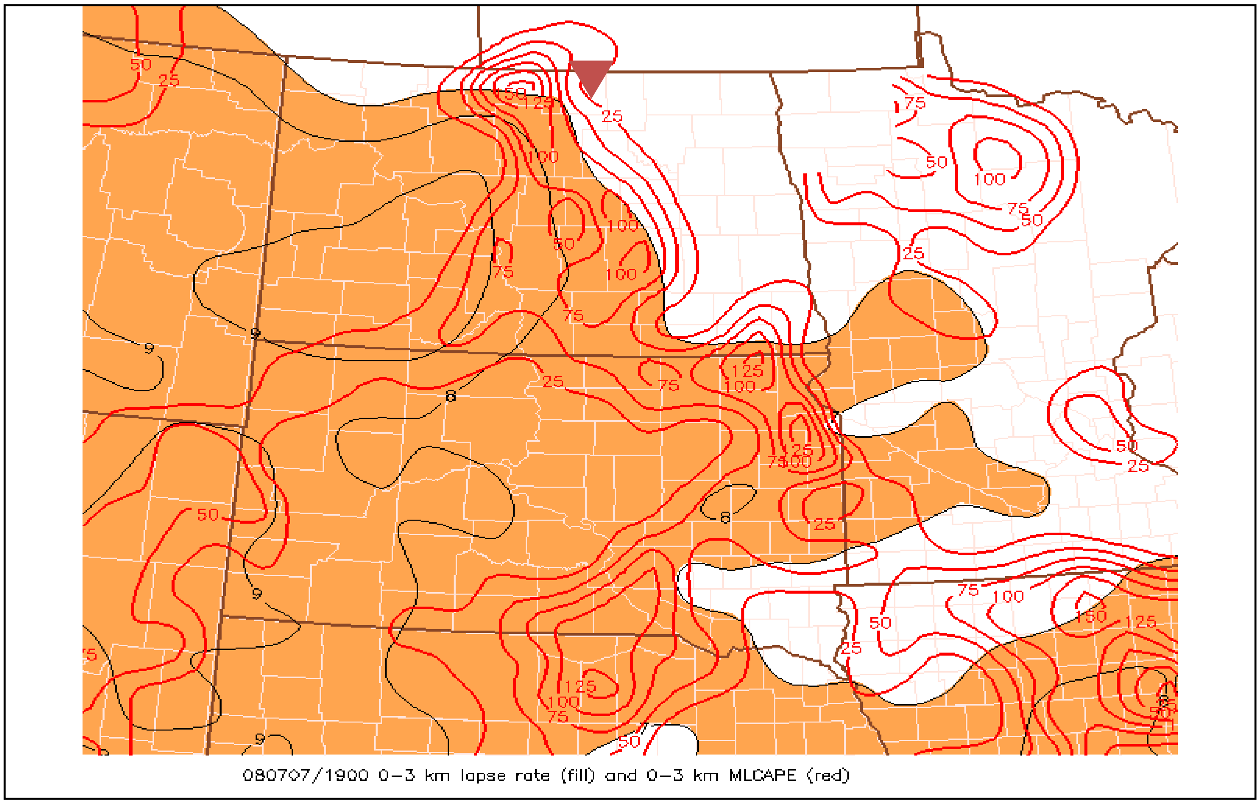

Figure 15. RUC analysis of 0–3-km temperature lapse rate (solid black contours, CI = 1°C km^{-1} for values beginning at 7°C km^{-1}, which is denoted by solid orange shading) and 0-3 km MLCAPE (solid red contours, CI = 25 J kg^{-1}) at 1900 UTC 7 July 2008. Location of EF3 tornado at 2030 UTC is denoted by a red inverted triangle.

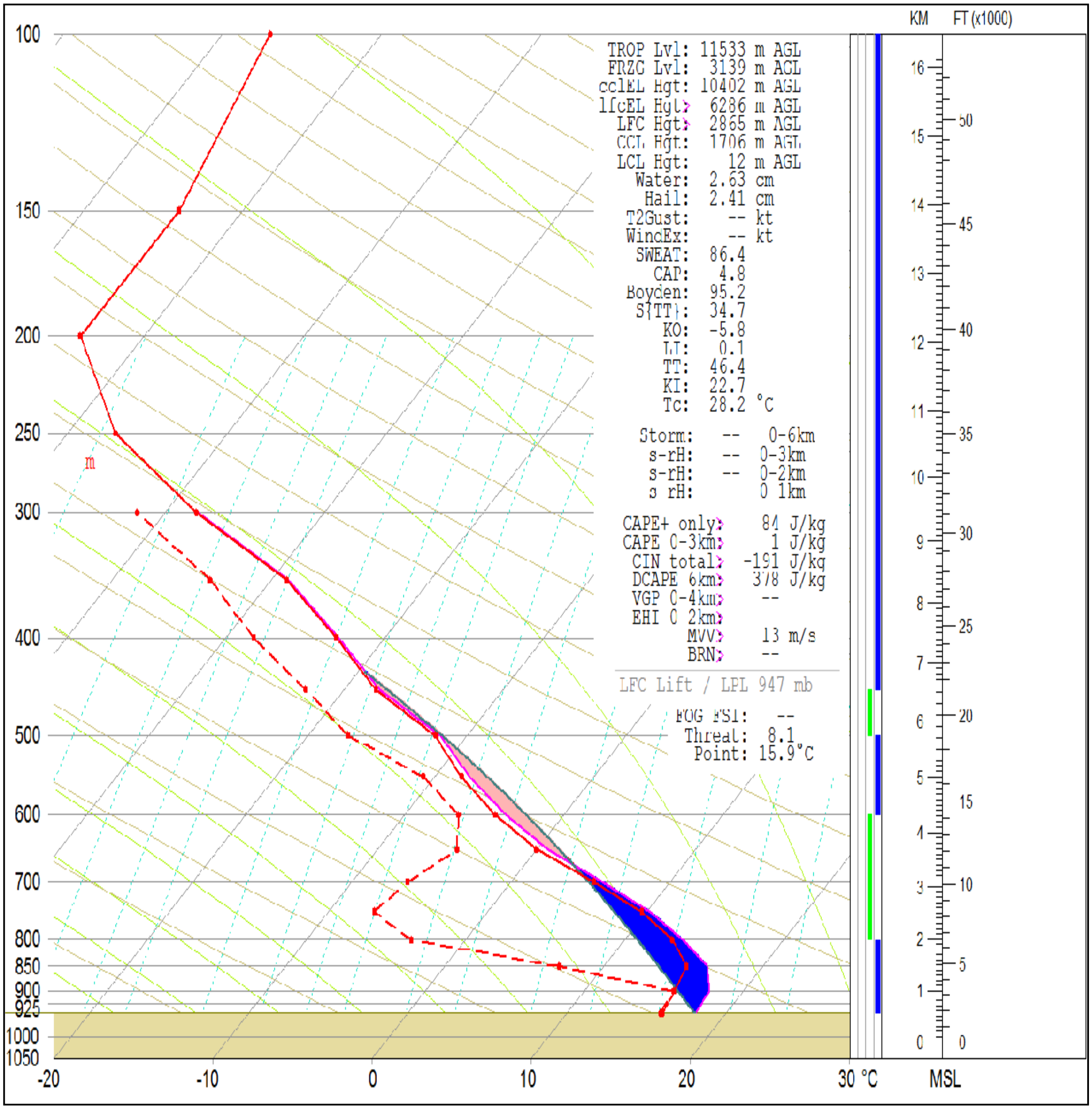

Fig. 16. Skew T–log P diagrams from a RUC analysis at Rolla, North Dakota at 1800 UTC 7 July 2008. Solid red line is the environmental temperature profile, red dashed line is the environmental dewpoint, solid pink line is the virtual temperature profile, and solid black line is the air parcel temperature. SBCAPE is shaded red. Dark red area represents the 0-3 km SBCAPE.

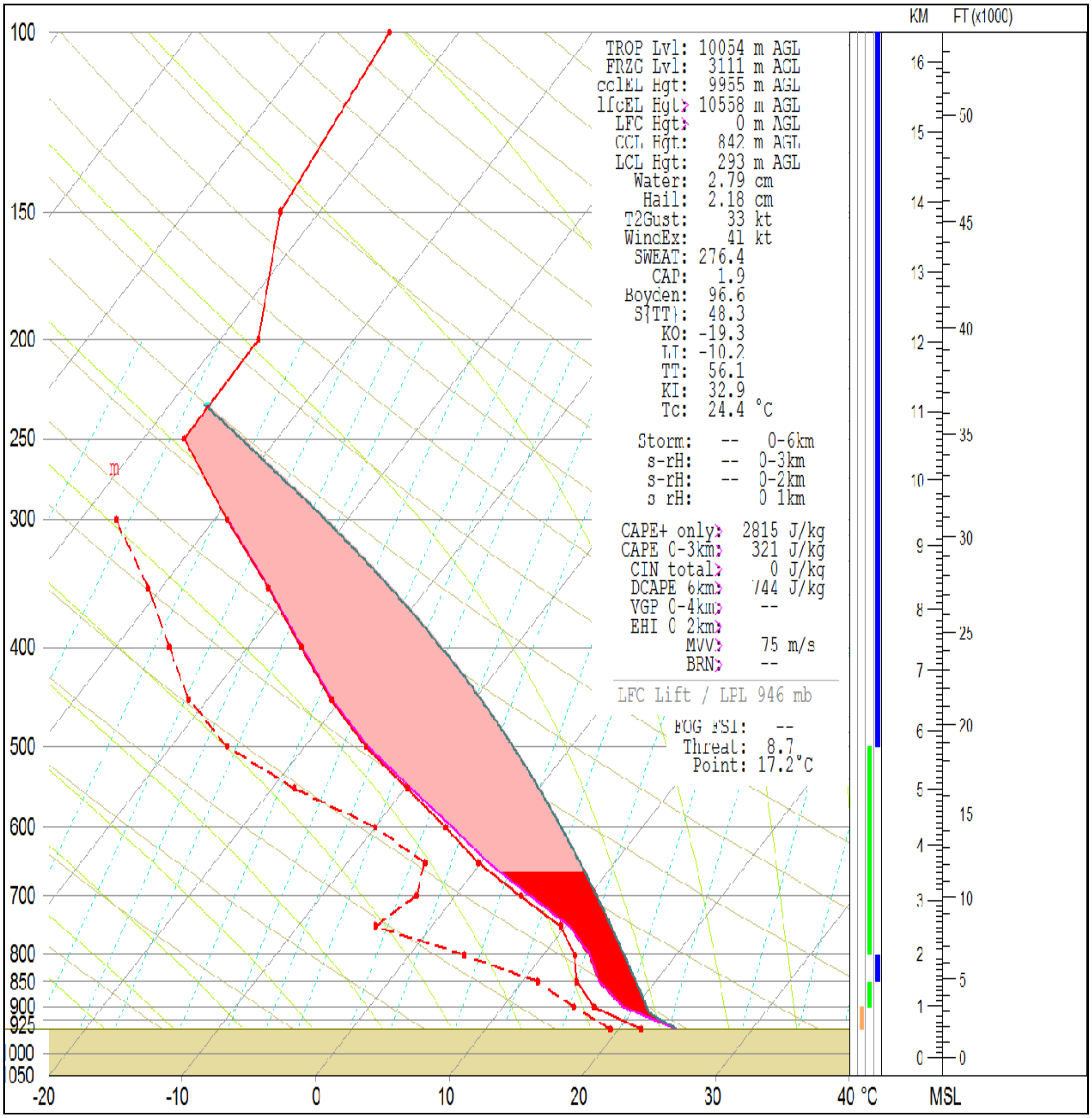

Figure 17. As in Fig. 16, but for 2000 UTC 7 July 2008.

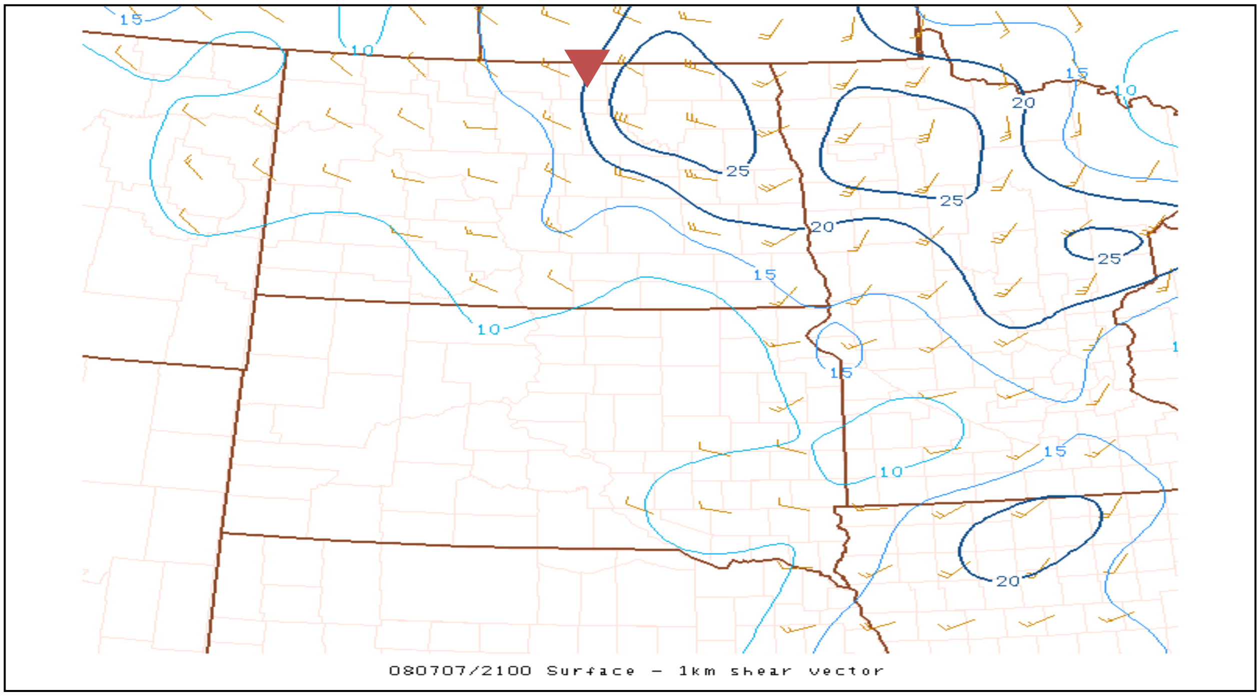

Figure 18. RUC analysis of 0–1-km bulk wind shear vectors and magnitude (solid blue contours, CI = 5 kt beginning at 10 kt) at 2100 UTC 7 July 2008. Location of EF3 tornado at 2030 UTC is denoted by a red inverted triangle.

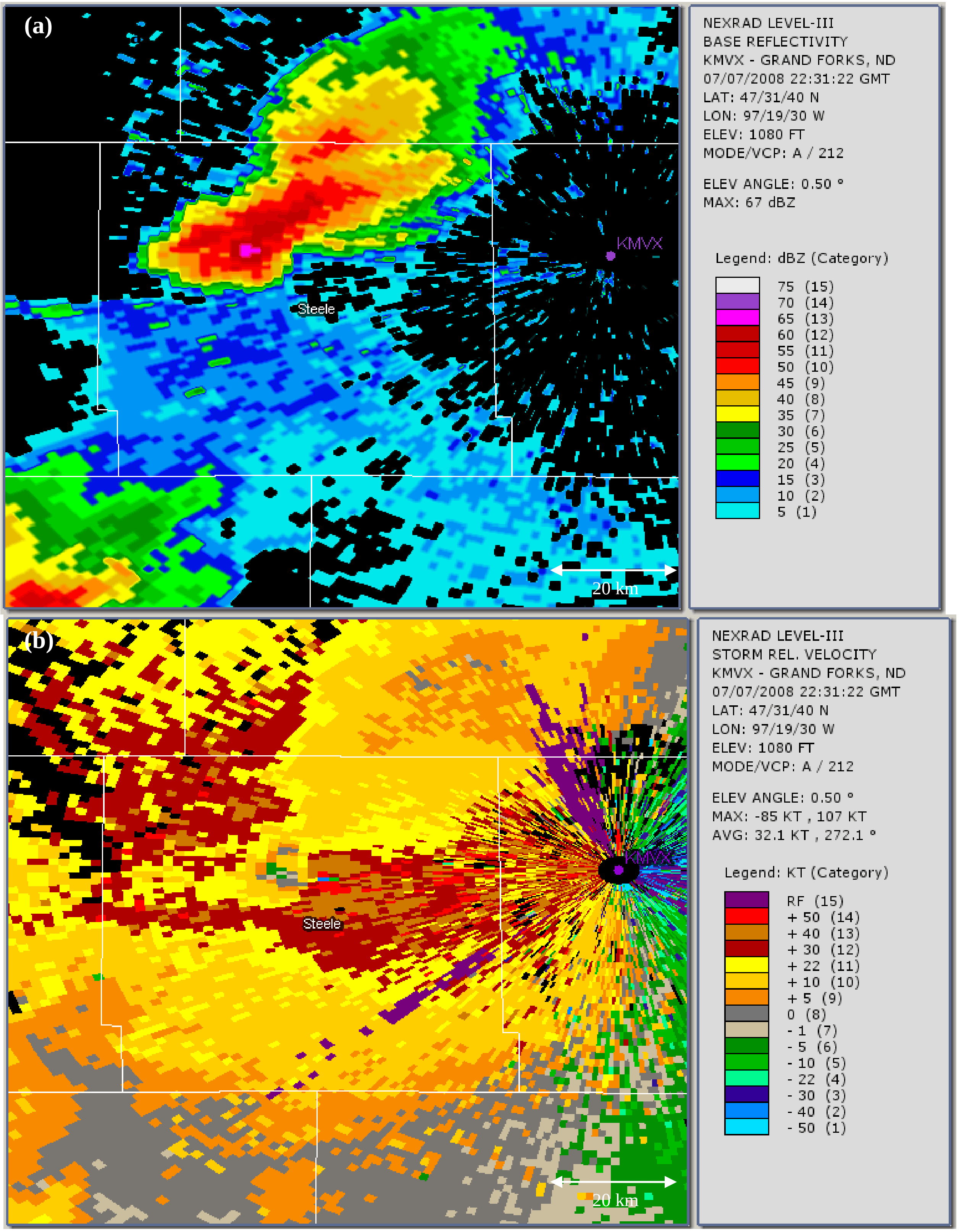

Figure 19. Mayville, North Dakota (KMVX) WSR-88D imagery at 2231 UTC 7 July 2008 for a) 0.5° radar reflectivity and b) 0.5° elevation storm-relative velocity. Click here for an animation of “a” and here for an animation of “b”.

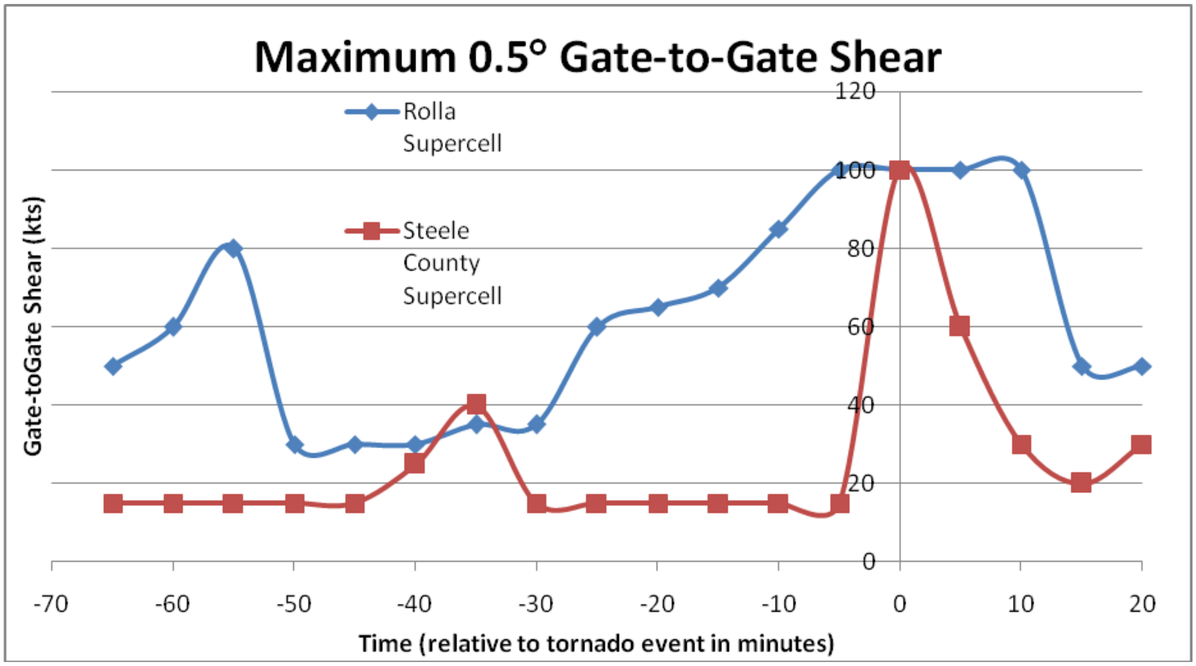

Figure 20. Maximum 0.5° elevation angle Gate-to-Gate shear trends of the Rolla supercell versus the Steele County supercell with respect to the tornado event time.

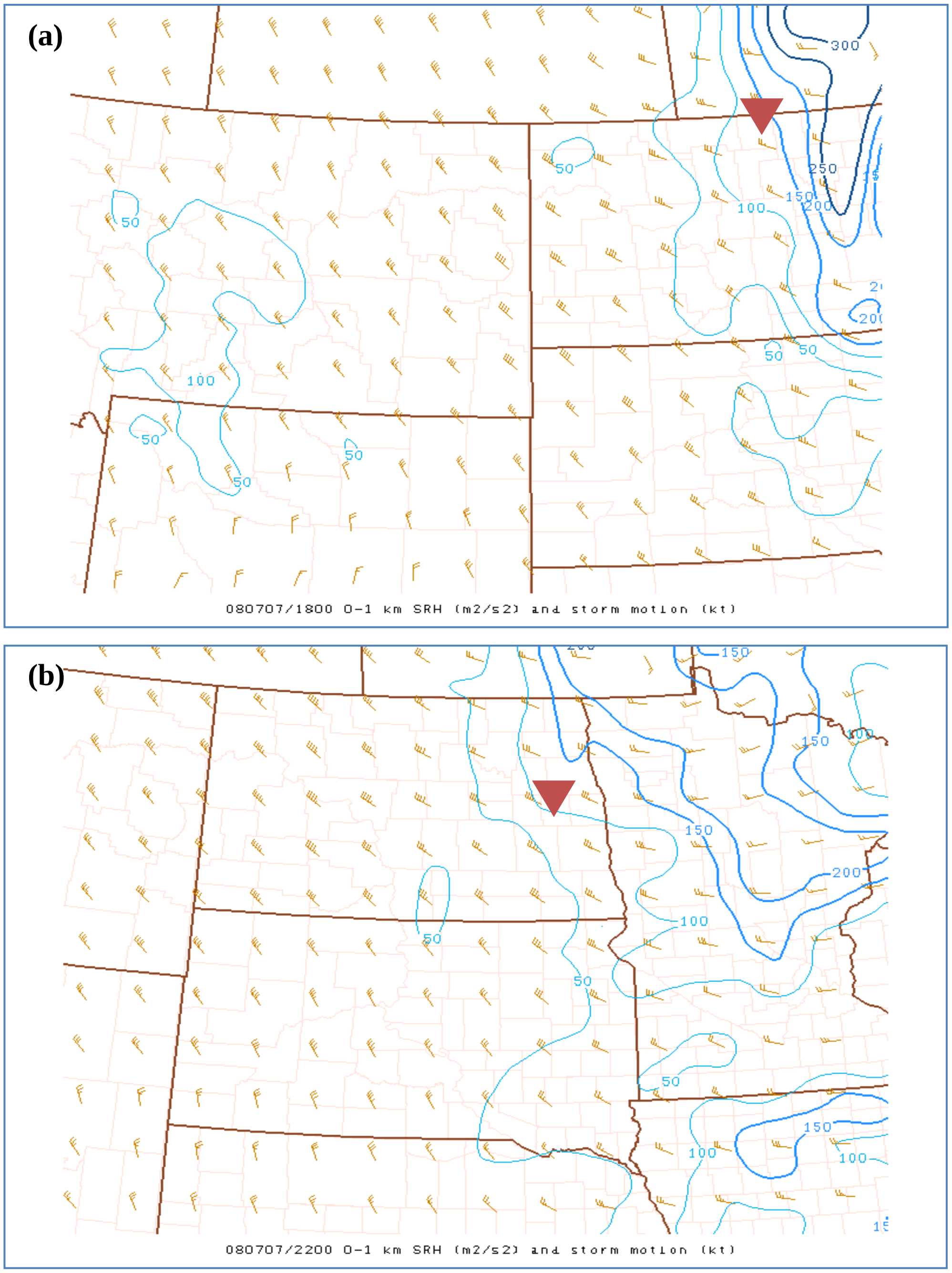

Figure 21. RUC analysis of 0–1-km storm-relative helicity (solid blue contours, CI = 50 $m^2 s^{-2}$) and storm motion vectors (conventional form) on 7 July 2008 at a) 1800 UTC and b) 2200 UTC. Red inverted triangles represent locations of a) the Rolla EF3 tornado at 2030 UTC and b) Steele County EF0 tornado at 2230 UTC.

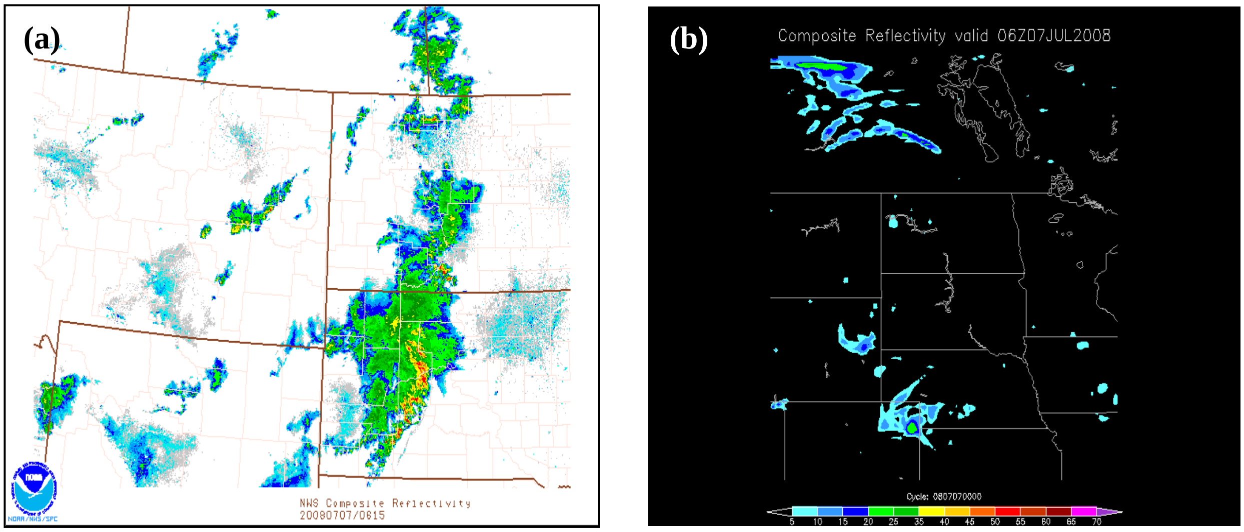

Figure 22. a) Regional WSR-88D composite reflectivity imagery at 0615 UTC 7 July 2008 and b) WRF-ARW 12-km HGS 06-hour simulated reflectivity forecast valid at 0600 UTC 7 July 2008.

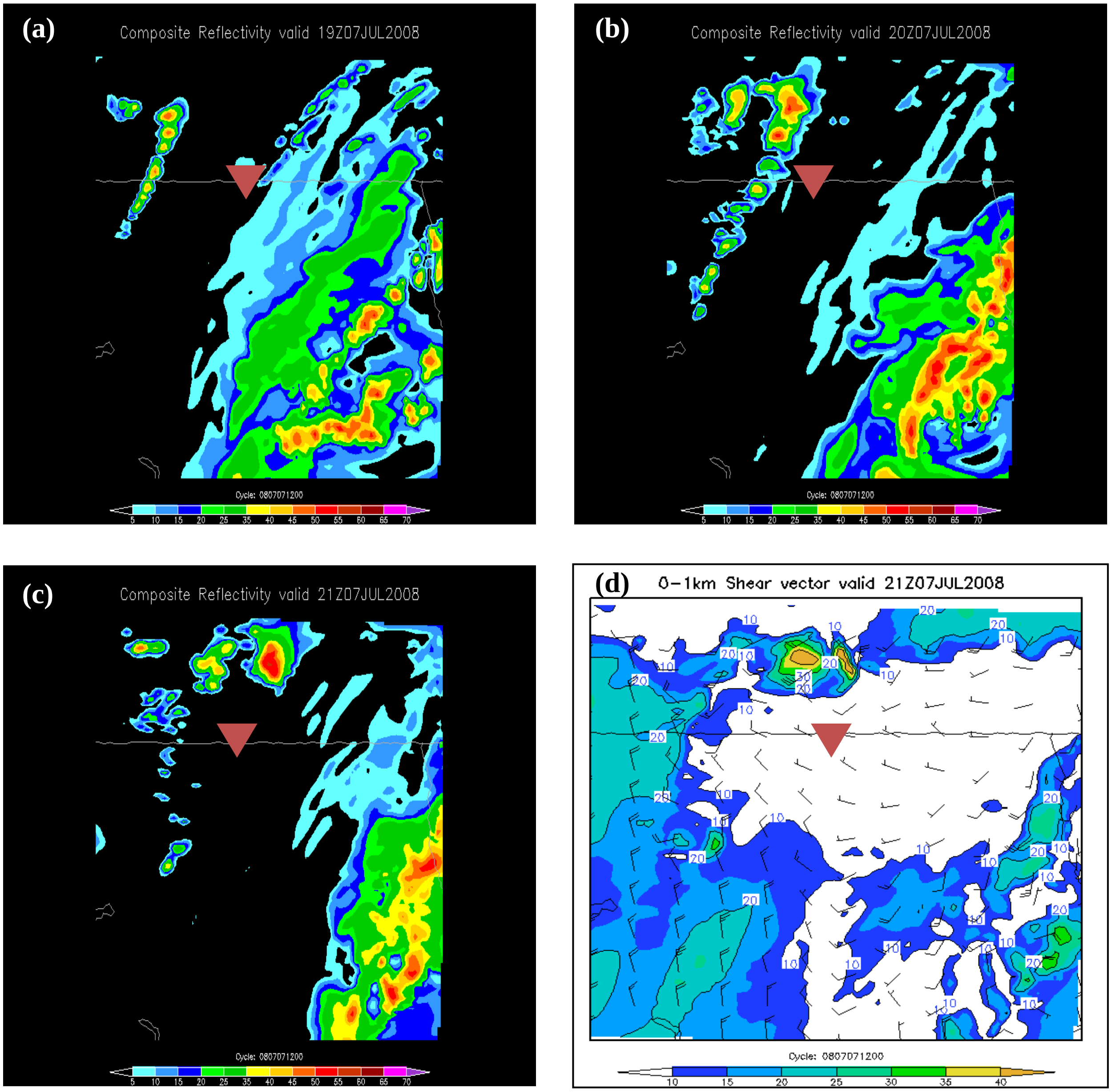

Figure 23. WRF-ARW 4-km HGS forecast of simulated reflectivity at a) 1900 UTC 7 July 2008, b) 2000 UTC 7 July 2008, and c) 2100 UTC 7 July 2008. d) 0–1-km bulk wind shear vectors and magnitude at 2100 UTC 7 July 2008 (solid contours and fill, CI = 10 kt). Inverted red triangle highlights the location of the Rolla, North Dakota EF3 tornado at 2030 UTC.